



# Kelvin Probe Force Microscopy of charged indentation-induced dislocation structures in KBr

P. Egberts and R. Bennewitz



## Abstract

The incipient stages of plasticity in KBr single crystals have been examined in ultrahigh vacuum by means of Atomic Force Microscopy and Kelvin Probe Force Microscopy (KPFM). Conducting diamond-coated tips have been used to both indent the crystals and image the resulting plastic deformation. KPFM reveals that edge dislocations intersecting the surface carry a negative charge similar to kinks in surface steps, while screw dislocations show no contrast. Weak topographic features extending in  $\langle 110 \rangle$  direction from the indentation are identified by atomic-resolution imaging to be pairs of edge dislocations of opposite sign, separated by a distance similar to the indenter radius. They indicate the glide of two parallel  $\{110\}$  planes perpendicular to the surface, a process that allows for a slice of KBr to be pushed away from the indentation site.

## Introduction

The fundamental study of the initial stages of plasticity is challenging as there are few instruments that combine the ability to quantify plastic deformation with accurate depth and force measurement, as well as acquire high resolution images of the deformed structure. A recent development is the increased use of Scanning Probe Microscopy (SPM) in the study of plasticity. It is supported by the wide distribution of instruments, the outstanding resolution of surface imaging [1-3], and additionally, the capability

of Atomic Force Microscopy (AFM) to measure forces with single-bond sensitivity [4-9]. The small contact radius of the probes used in SPM allows for the application of large stresses at small applied loads. Furthermore, the use of SPM probes as indenters can produce localized indentations, where the plastic zone can be confined between a few micrometers down to a few nanometers. Such small areas can be imaged beforehand to identify regions where the indented volume can be considered to be of perfect crystallinity, free from pre-existing dislocations. In these regions, plasticity must be accommodated by homogeneous nucleation of dislocations rather than activation of Frank-Read sources [10]. Incipient plasticity has now been studied using SPM for indentation and imaging on a number of surfaces, including MgO(100) [5], Au(100) [2-4], Au (111) [4, 6], KBr (100) [7], Cu (100) [8], and stepped Au surfaces [9], in both ambient and ultrahigh vacuum conditions.

Plastic deformation of ionic crystals is often closely connected with charge movement within the crystals and a build-up of charge on their surfaces. For example, the application of a large electric field to KCl(100) during indentation was found to affect the movement of edge dislocations in a way that allowed assignment of a negative charge to edge dislocations [11]. In contrast, the movement of screw dislocations was not affected by the electric field, indicating that they carry no charge. However, when alkali halides are doped with divalent cations, edge

dislocations were found to be negatively charged [12]. Charge compensation of divalent impurities has also been studied by Barth and Henry. They found that kink sites on the surface produced in the cleavage process trap cation vacancies. The result is a negatively charged surface and a positive space charge of divalent cations below the surface that together forms the surface double layer [13]. Barth and Henry identified kink sites as charge traps by means of Kelvin Probe Force Microscopy (KPFM). In the present study, we use KPFM to study the topography and the charges on surfaces plastically deformed in indentation experiments, using the same tip for indentation and imaging. An extended version of this article will appear as Ref. [14].

### Experimental Techniques

For all experiments, a home-built AFM with optical beam deflection method for force detection [15] was used in both contact and non-contact modes. The experiments were performed in ultra-high vacuum (UHV) at room temperature and at a pressure of  $< 2 \times 10^{-10}$  mbar. Single crystals of KBr were cleaved along the (100) surface in air and introduced into the UHV chamber immediately. The crystals were then heated for 1 hour at 120 °C to remove charges and surface contaminants. The main impurities in the crystal were found by mass spectrometry to be 93 mg/kg of Na and 6 mg/kg of Ca. The KBr(100) surface was imaged by non-contact AFM [16] and by frequency-modulated KPFM [17]. Once a suitable

area for indentation was found, the oscillation of the cantilever was stopped and the surface indented until dislocation activity was detected. Following indentation, the surface topography and charges were imaged again.

### Kelvin Probe Force Microscopy of Indentations

Figure 1 shows typical topographic and KPFM maps of a surface area selected for an indentation experiment. The topography includes a defect-free atomically flat

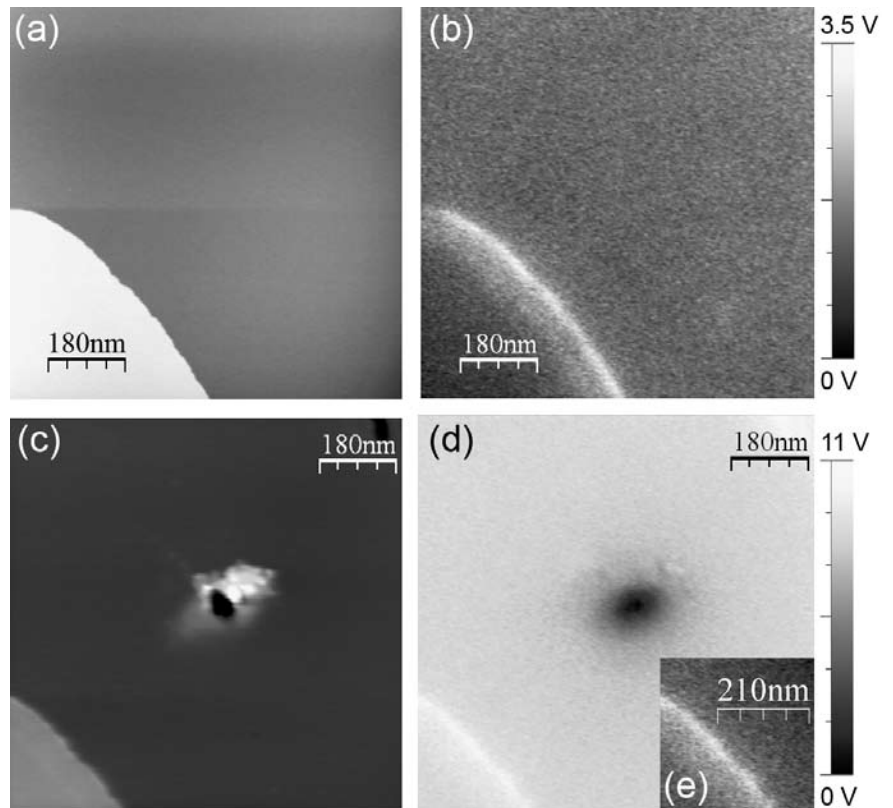


Figure 1: Topographic (a) and KPFM map (b) of an atomically flat terrace and a monatomic step on KBr(001) before indentation. Topographic (c) and KPFM map (d) after indentation of the same area. The KPFM map in inset (e) is a detail of (d) using the same colour scale as in (b), demonstrating that polarity and magnitude of the KPFM signal over the curved step edge remains the same.



terrace and a monatomic curved cleavage step. This variation in the KPFM signal over the curved step edge, which shows a positive contrast compared to the surrounding terraces, is used as a reference of the surface charge before and after indentation. The positive contrast indicates that there is a high density of negatively charged kink sites at this step edge. The surface area after indentation is shown in Figure 1 (c-e). The topography exhibits a depression at the site of indentation, some elevated material around the indentation, and a string of weak features extending from the indentation toward the upper left corner of the frame. The KPFM map shows several common features observed after indentations in KBr(100). The indentation site itself shows a strong negative KPFM signal while the KPFM signal over the curved step edge next to the indent maintains the same magnitude and polarity as was observed before indentation, as demonstrated by Figure 1(e) which uses the same colour scale as Figure 1(b). This result confirms that the conducting diamond-coated tip does not change its properties with respect to the KPFM signal during the indentation. All indents studied by KPFM using different diamond tips were observed to require a negative applied bias of several volts at the site of indentation, revealing significant positive charges in the indents.

### Edge Dislocations in KBr

The stress caused by the indentation has a component parallel to the surface and the KBr crystal has an active glide sys-

tem parallel to the surface, namely in the  $\{110\}\langle 110\rangle$  glide system. If glide parallel to the surface is activated, then no new surface steps are created and the glide of edge dislocations, whose Burgers vectors have no component normal to the surface, is initiated. Consequently, glide planes and edge dislocations have no topographic characteristic at the surface and are difficult to detect by non-contact AFM. In this section we will show that the string of weak features observed in Figure 1(c) are edge dislocations.

Figure 2(a) gives a magnified topographic view of the features from Figure 1(c). The height of an individual hillock is 0.051 nm, clearly less than one atomic step. Figure 2(c) reveals the atomic configuration of one of the hillocks from Figure 2(a). We find two edge dislocations, one at the upper right end of the hillock, and one at the lower left.

The topographic image at higher magnification of an edge dislocation in Figure 2(d) shows how the Burgers vector of an edge dislocation was determined. Following a square of equal side length in units of distinctly visible atoms, the Burgers vector is given as the vector closing the square. For this dislocation, the Burgers vector has a magnitude of  $\sqrt{2}a/2$  in the  $[1-10]$  direction, as expected for an edge dislocation intersecting the (100) surface. Using the same method, the two Burgers vectors can be determined for the hillock in Figure 2(c). At the end of the hillock labelled *I*, the Burgers vector points in the  $[1-10]$  direction, and at the end of the hillock labelled *II* the Burg-

ers vector points in the  $[-110]$  direction, both having the same magnitude of  $\sqrt{2}a/2$ . The distance between the dislocations is 28 atomic protrusions, or 9.28 nm. Note the close agreement between the width of the hillocks and the tip radius estimated earlier to be 11 nm.

Figure 2(b) shows the KPFM signal recorded together with Figure 2(a). The individual hillocks are not resolved, although there is a path of positive KPFM signal along the  $\langle 110 \rangle$  direction from the indentation site in the direction where hillocks are observed in the topography. This result is in contrast to the lack of KPFM contrast for screw dislocations and indicates that the edge dislocations carry a negative charge similar to the kink sites in step edges.

## Conclusion

In summary, we have demonstrated that Kelvin Probe Force Microscopy is a suitable tool to detect charges of dislocations at surfaces of insulating crystals. Diamond-coated tips have been used to nucleate few dislocations and analyze the resulting surface structure including atomic resolution of pairs of edge dislocations. Edge dislocations in KBr containing traces of divalent impurities carry negative charge similar to kinks in monatomic steps, while screw dislocation show no contrast in KPFM. Two mechanisms of material transfer away from the indentation site are observed: glide initiated normal to the surface followed by multiple cross-slips creates a complex

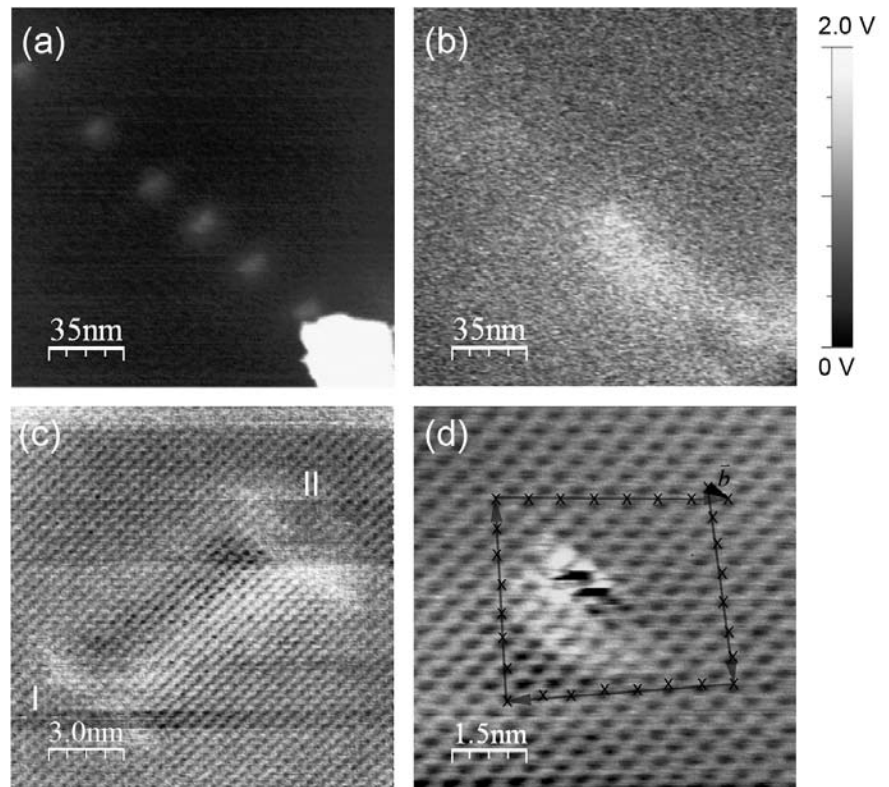


Figure 2: Higher magnification topographic (a) and KPFM map (b) of the string of shallow hillocks emerging from the surface during the indentation shown in Figure 1. Atomic resolution of an entire hillock (c) and of the edge dislocation at one end of a hillock (d). The Burgers circuit drawn on (d) illustrates the direction and magnitude of the Burgers vector for this edge dislocation.

structure of monatomic islands in the vicinity of the indentation and initiation of glide parallel to the surface allowing for movement of slices of material towards the  $\langle 110 \rangle$  direction, resembling the classical rosette pattern.

This study has been carried out at McGill University, Montreal (Canada) and the INM. The work was supported by the Canada Foundation of Innovation and Natural Sciences and Engineering Research Council (NSERC). The chemical analysis of the crystals by Claudia Fink-



Straube and Andrea Jung at the INM are gratefully acknowledged.

## References

- [1] J. de la Figuera, M. A. González, R. García-Martínez, J. M. Rojo, O. S. Hernán, A. L. Vázquez de Parga, R. Miranda, *Phys. Rev. B*, 1998, 58, 1169-1172.
- [2] E. Carrasco, O. Rodríguez de la Fuente, M. A. González, J. M. Rojo, *Phys. Rev. B*, 2003, 68, 180102.
- [3] E. Carrasco, M. A. González, O. Rodríguez de la Fuente, J. M. Rojo, *Surf. Sci.*, 2004, 572, 467-475.
- [4] J. D. Kiely, J. E. Houston. *Phys. Rev. B*, 1998, 57, 12588-12594.
- [5] P. F. M. Terán Arce, G. Andreu Riera, P. Gorostiza, F. Sanz, *Appl. Phys. Lett.*, 2000, 77, 839-841.
- [6] A. Asenjo, M. Jaafar, E. Carrasco, J. M. Rojo, *Phys. Rev. B*, 2006, 73, 75431.
- [7] T. Filleter, S. Maier, R. Bennewitz, *Phys. Rev. B*, 2006, 73, 155433.
- [8] T. Filleter, R. Bennewitz, *Nanotechnology*, 2007, 18, 044004.
- [9] V. Navarro, O. Rodríguez de la Fuente, A. Mascaraque, J. M. Rojo, *Phys. Rev. Lett.*, 2008, 100, 105504.
- [10] D. Lorenz, A. Zeckzer, U. Hilpert, P. Grau, H. Johansen, H. S. Leipner, *Phys. Rev. B*, 2003, 67, 172101.
- [11] L. Colombo, T. Kataoka, J. C. M. Li, *Phil. Mag. A*, 1982, 46, 211-215.
- [12] M. R. Dalmau, A. Paz, J. A. Gorri, *Phys. Stat. Sol. A*, 1986, 96, 533-540.
- [13] C. Barth, C. R. Henry, *Phys. Rev. Lett.*, 2007, 98, 136804.
- [14] P. Egberts, T. Filleter, R. Bennewitz, *Nanotechnology*, 2009, in print.
- [15] L. Howald, E. Meyer, R. Lüthi, H. Haefke, R. Overney, H. Rudin, H.-J. Güntherodt, *Appl. Phys. Lett.*, 1993, 63, 117-119.
- [16] F. J. Giessibl, In: S. Morita, R. Wiesendanger, E. Meyer, Eds., *Noncontact Atomic Force Microscopy*, Springer: Berlin, 2002, 11-46.
- [17] M. Nonnenmacher, M. P. O'Boyle, H. K. Wickramasinghe, *Appl. Phys. Lett.*, 1991, 58, 2921-2923.